

Why is the electrocaloric effect so small in ferroelectrics?

G. G. Guzmán-Verri^{1,2} and P. B. Littlewood^{3,4}

¹*Materials Science Division, Argonne National Laboratory, Argonne, Illinois, USA 60439*

²*Centro de Investigación en Ciencia e Ingeniería de Materiales,
Universidad de Costa Rica, San José, Costa Rica 11501*

³*Argonne National Laboratory, Argonne, Illinois, USA 60439*

⁴*James Franck Institute, University of Chicago, 929 E 57 St, Chicago, Illinois, USA 60637*

(Dated: October 1, 2022)

Ferroelectrics are attractive candidate materials for environmentally friendly solid state refrigeration free of greenhouse gases. Their thermal response upon variations of external electric fields is largest in the vicinity of their phase transitions, which may occur near room temperature. The magnitude of the effect, however, is too small for useful cooling applications even when they are driven close to dielectric breakdown. Insight from microscopic theory is therefore needed to characterize materials and provide guiding principles to search for new ones with enhanced electrocaloric performance. Here, we derive from well-known microscopic models of ferroelectricity meaningful figures of merit for a wide class of ferroelectric materials. Such figures of merit provide insight into the relation between the strength of the effect and the characteristic interactions of ferroelectrics such as dipolar forces. We find that the long range nature of these interactions results in a small effect. A strategy is proposed to make it larger by shortening the correlation lengths of fluctuations of polarization. In addition, we bring into question other widely used but empirical figures of merit and facilitate understanding of the recently observed secondary broad peak in the electrocalorics of relaxor ferroelectrics.

The thermal changes that occur in ferroelectric (FE) materials upon the application or removal of electric fields are known as the electrocaloric effect (ECE).^{1–7} The effect was first studied in Rochelle salt in 1930⁸ and it's the electric analogue of the magnetocaloric effect, which is commonly used to reach temperatures in the milliKelvin range. The ECE is the result of entropy variations with polarization, e.g., isothermal polarization of a ferroelectric reduces its entropy while depolarization increases it. It is parametrized by isothermal changes in entropy ΔS and adiabatic changes in temperature ΔT and it is strongest near the ferroelectric transition.

Since the phase transitions occur near room temperature in many FEs, the potential for using the ECE for cooling applications is huge: it could provide an alternative to standard refrigeration technologies based on the vapor-compression method in which the running substances are greenhouse gases such as freon and hydrochlorofluorocarbons;⁹ replace the widely used but inefficient small thermoelectric cooling devices such as Peltier coolers;² and lead to energy harvesting applications.¹⁰ Moreover, developing cooling prototypes based on the ECE^{11–13} may have several advantages over those based on the more studied magnetocaloric effect as the magnetic materials of interest require expensive rare-earth elements and large magnetic fields, while many FEs are ceramics or polymers, which are cheap and can be driven with electric fields that are easy to generate.

Though promising, a major challenge is that the magnitude of the ECE remains too small for useful applications: in bulk FEs, ΔT is usually less than a few milliKelvin per Volt and ΔS is usually a fraction of a $\text{JK}^{-1}\text{mol}^{-1}$.² FE thin films exhibit ECEs of about an order of magnitude larger than their bulk counterparts

as they can withstand larger breakdown electric fields.¹⁴ Thin films, however, have small cooling power because of their small heat capacities. Ferroelectric polymers have also received considerable attention with ECEs comparable to those of thin films, though they must be driven at larger electric fields than those of thin films.¹⁵

In the light of these challenges, it has been recently pointed out that insight from microscopic theory into the ECE may contribute to characterize known materials and provide guiding principles to search for new ones with enhanced electrocaloric performance.² Here, we provide such insight by deriving meaningful figures of merit from well-known microscopic models of ferroelectricity. Our figure of merit allow us to set trends across different classes of FE materials (order-disorder and displacive) and provides insight into the relation between the magnitude of the ECE and the characteristic interactions of FEs (e.g. dipolar and strain). We find that the long-range nature of these interactions produces trade-offs in the ECE: while they can give rise to high transition temperatures (i.e., comparable to room temperature), they concomitantly give rise to long correlation lengths of polarization at finite electric fields, which, as we show here, result in a small effect. We make contact with well-known results derived from Landau theory¹⁶ and those from heuristic arguments.¹⁷ Based on these findings, we then study the effects of compositional disorder. The purpose of this is twofold: to propose a strategy to increase the magnitude of the ECE and to model the ECE of so-called relaxor ferroelectrics - a widely studied class of electrocaloric materials with diffuse phase transitions that could provide a broad temperature range of operation in a cooling device.^{17–29} We find that the commonly observed secondary broad peak in the ECE of relaxors^{20,28} is expected in any ferroelectric that is

deep in the supercritical region of their phase diagram. Our results also bring into question the common practice of defining the electrocaloric strength of a material as the ratio of the entropy or temperature changes over the change in applied electric field.^{2,5}

To illustrate the ideas presented above, we adhere to a simple microscopic model for displacive ferroelectrics with quenched random electric fields.³⁰ Such compositional disorder is typical of relaxor ferroelectrics such as the prototype $\text{PbMg}_{1/3}\text{Nb}_{2/3}\text{O}_3$ (PMN) and it arises from the different charge valencies and disordered location of the Mg^{+2} and Nb^{+5} ions. In the absence of disorder, it is a standard minimal model of ferroelectricity.¹⁶ With disorder, the model gives a good starting point for the description of the static dielectric properties of relaxors.^{30,31}

In calculating the ECE in the presence of compositional disorder, it is important to recall that Maxwell relations are not applicable. Maxwell relations are usually invoked in ferroelectrics to indirectly determine, for instance, adiabatic changes in temperature ΔT from the variations of the polarization with respect to temperature.⁵ Pure ferroelectrics are in thermodynamic equilibrium, thus Maxwell relations hold. Disordered ferroelectrics are not in thermodynamic equilibrium, thus Maxwell's relations do not apply. This is supported by the recent experimental observation that direct measurements of ΔT in solutions of the relaxor ferroelectric polymer PVDF-TrFE-CFE with PVDF-CTFE were significantly larger than those estimated from their polarization curves.²² Another difficulty is that Landau theory fails for relaxors. Landau theory is applicable away from the region of critical fluctuations of polarization that occur near the transition point. In conventional ferroelectrics, Landau theory works remarkably well since this region is narrow.¹⁶ In relaxors, on the other hand, Landau theory is not expected to hold as the region of critical fluctuations is broad. We overcome both of these difficulties by calculating the ECE directly from the entropy function (see supplement).

We first consider the case without compositional disorder. In the absence of disorder and no applied electric field, the model gives a second-order paraelectric-to-ferroelectric phase transition at a transition temperature T_c^0 . Consider an isothermal change in entropy $\Delta S(T, E_0)$ near T_c^0 that results from a change in electric field $\Delta E_0 = 0 \rightarrow E_0$. Within a mean field approximation, we find that

$$\frac{|\Delta S(T, E_0)|}{Nk_B} = (2\pi\zeta a^2/3) [\xi^{-2}(T, E_0) - \xi^{-2}(T, 0)]. \quad (1)$$

where ζ is a dimensionless coefficient that depends on the lattice structure, a is the lattice constant and N is the number of lattice sites.³⁰ $\xi(T, E_0)$ is the correlation length of the exponentially decaying fluctuations of polarization at the field E_0 and temperature T .¹⁶ It

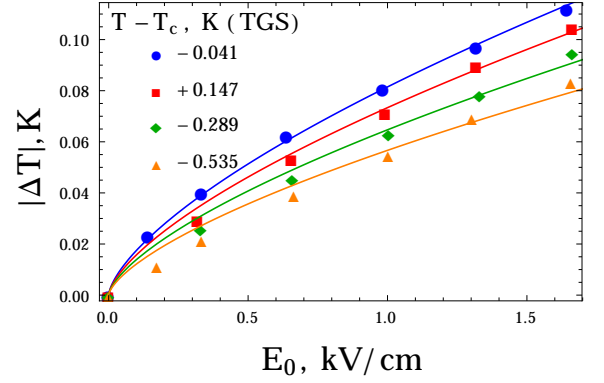


FIG. 1. Applied electric field dependence of the adiabatic changes in temperature near the paraelectric-to-ferroelectric transition ($T_c \simeq 322$ K) in triglycine sulphate (TGS). Solid lines correspond to fits to the electric field to the power of $2/3$ as predicted by Eq. (3). Data taken from Ref. [32].

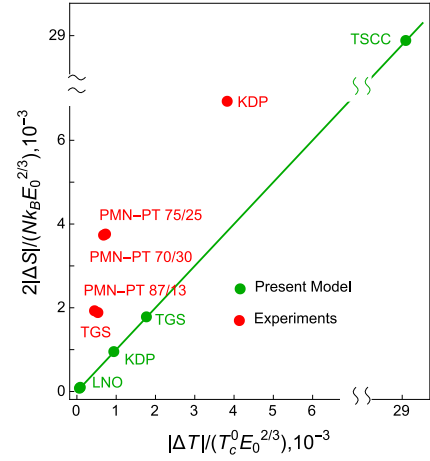


FIG. 2. Figure of merit at the paraelectric-to-ferroelectric transition for several ferroelectrics according to Eq. (3). Axes are in units of $(\text{statvolt}/\text{cm})^{2/3}$. Here, TSCC = $(\text{CH}_3\text{NHCH}_2\text{COOH})_3\text{CaCl}_2$, KDP = KH_2PO_4 , TGS = $(\text{NH}_2\text{CH}_2\text{COOH})_3 \cdot \text{H}_2\text{SO}_4$, LNO = LiNbO_3 , and PMN-PT $1-x/x = (\text{PbMg}_{1/3}\text{Nb}_{2/3}\text{O}_3)_{1-x}(\text{PbTiO}_3)_x$. Data taken from Refs. [2, 32, 35].

is given by the (soft) frequency of the transverse optic phonon mode³⁰ and it diverges as $\xi(0, T) \propto (|T - T_c|)^{-1/2}$ at the onset of the FE transition.¹⁶ A similar relation is derived for the adiabatic changes in temperature $\Delta T(T_1, E_0) = T_2 - T_1$,

$$\frac{\Delta T(T_1, E_0)}{T_1} = (\pi\zeta a^2/3) [\xi^{-2}(E_0, T_2) - \xi^{-2}(0, T_1)]. \quad (2)$$

Equations (1) and (2) relate the ECE to the correlation length of a ferroelectric. We make contact with known results by noting that near the FE transition, $(\xi(T, E_0)/a)^{-2} - (\xi(T, 0)/a)^{-2} \simeq (\zeta k_B n)^{-1} P_s^2(T, E_0)/C_{CW}$ in Eqs. (1), which gives the

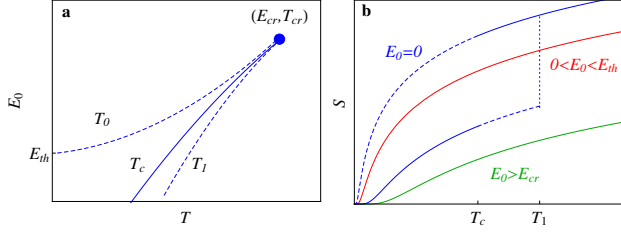


FIG. 3. (a) Schematic of the electric field-temperature phase diagram for ferroelectric with disorder. The coexistence line (blue) ends at a critical point (E_{cr}, T_{cr}) . Spinodal curves T_0 and T_1 indicate the end of the stability of the paraelectric and ferroelectric states, respectively. (b) Schematic entropy-temperature phase diagram for various electric field regimes. Solid and dashed lines correspond to stable and metastable states, respectively. The entropy function for $E_{th} < E_0 < E_{tr}$ is not shown for clarity.

standard results from Landau theory¹⁶ and similar form to those derived from heuristic arguments.¹⁷ $P_s(T, E_0)$ is the polarization at temperature T and at field E_0 , C_{CW} is the Curie-Weiss constant, and $n = N/V$ is the number of lattice points per unit volume V . At the phase transition, $\Delta S(T_c^0, E_0)$ and $\Delta T(T_c^0, E_0)$ of Eqs. (1) and (2) peak as the correlation length at zero field diverges ($\xi(T_c^0, 0) = \infty$) and their magnitude depends on that at finite fields. For ferroelectrics, it is well-known that these tend to be large due to the long-range nature of the dipole and strain interactions.¹⁶

We now derive our figure of merit. By evaluating the correlation length at the critical temperature ($\xi^{-2}(E_0, T_c^0) \propto (T_c^0/C_{CW})^{1/3} (E_0/P_s^0)^{2/3}$) in Eqs. (1) and (2), we obtain the magnitude of the ECE in terms of dielectric properties of a FE,

$$\frac{\Delta T(T_c^0)}{T_c^0} \simeq \frac{\Delta S(T_c^0)}{Nk_B/2} \propto \left(\frac{T_c^0}{C_{CW}} \right)^{1/3} \left(\frac{E_0}{P_s^0} \right)^{2/3}, \quad (3)$$

where $P_s^0 = P_s(0, 0)$ is the saturated polarization at zero field. The coefficient of proportionality is a dimensionless number $((81/(4\pi))^{2/3} \simeq 1.7)$. Eq. (3) is our figure of merit.

The available data confirm the non-linearity predicted by our simple model: figure 1 shows that $\Delta T \propto E_0^{2/3}$ near the ferroelectric transition of triglycine sulphate (NH₂CH₂COOH)₃·H₂SO₄ (though TGS is a ferroelectric of the order-disorder type, it is straightforward to show that $\Delta T(T_{CW})/T_{CW} = (9/4\pi)^{2/3} (E_0/P_s^0)^{2/3}$, therefore its ECE scales with the electric field as in Eq. (3)). Similar scaling laws have been observed in the magnetocaloric effect.³³ The non-linearity in E_0 suggests that it is not meaningful to define $\Delta S/\Delta E_0$ or $\Delta T/\Delta E_0$ as the electrocaloric strength of an electrocaloric material when ΔS and ΔT are measured near or at the transition temperature.^{2,5}

From Eq. (3) and data from the literature,³⁴ we calculate our figure of merit for several FE materials. The results are shown in Figure 2. Our model predicts a clear trend: order-disorder FEs should display larger ECE than that of the displacive type. This is a consequence of the shorter correlation lengths that the former type generally display compared to those of the latter type (order-disorder Curie-Weiss constants are typically about two orders of magnitude smaller than those of displacive FEs). An exception to this rule may exist, however, in the ultraweak displacive FEs such as tris-sarcosine calcium chloride (TSCC). Our predicted figure of merit is an order of magnitude larger than any of the FEs considered here as a result of their exceptionally small Curie-Weiss constants and spontaneous polarization (which result in shorter correlation lengths).³⁵ The ECE has been recently measured in brominated TSCC compounds, however, we cannot compare to our model as the measurement was performed near its quantum critical point.³⁶ When Eq. (3) is contrasted to experiments,² there are clear discrepancies which we attribute to the mixed order-disorder and displacive character that most FEs display, and to their large anharmonicities (beyond quartic order). These differences, though, are not too severe specially when considering the simplicity of the model.

We now consider the effects of compositional disorder. Following Ref. [30], we parametrize the quenched random electric fields by a Gaussian probability distribution with zero mean and variance Δ^2 (see supplement). Figures 3 (a)-(b) show a schematic of the electric field-temperature ($E - T$) phase diagram and the entropy function for moderate disorder. There are metastable paraelectric states with a stability region that extends to zero temperature. Ferroelectric states appear as local minima in the free energy at high temperatures and become stable below a coexistence temperature $T_c < T_c^0$. The coexistence line of the polar and non-polar phases ends at a critical point (T_{cr}, E_{cr}) . Weak first-order phase transitions are induced for electric fields greater than a threshold field E_{th} as they cross the region of stability of the metastable paraelectric phase. For fields smaller than E_{th} , no macroscopic ferroelectric transition occurs with a spontaneous polarization. In typical relaxors such as PMN, $E_{th} \simeq 2$ kV/cm and $(T_{cr}, E_{cr}) \simeq (240 \text{ K}, 4 \text{ kV/cm})$.³⁷

Figures 4(a)-(d) show the electric field and temperature dependences of the ECE for zero and moderate disorder. In both cases the peaks in ΔS and ΔT occur at their corresponding transition temperatures and increase monotonically with increasing applied field, as expected. For moderate disorder, however, ΔS increases provided the applied field is greater than E_{th} . This increment occurs because of the shortening of the correlation length, as indicated by Eq. (3). Though ΔT is also affected by the shortening of the correlation length, it decreases with disorder as T_c shifts to lower temperatures. We emphasize here that we are refering

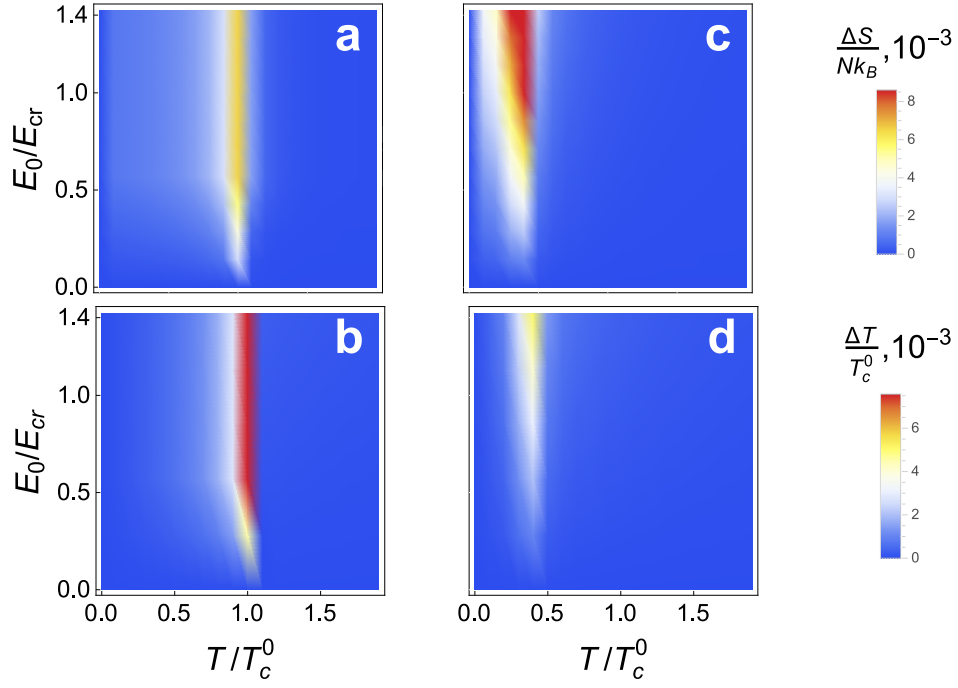


FIG. 4. Density plots of the adiabatic changes in temperature and isothermal changes in entropy for (a)-(b) no and (c)-(d) moderate $((\Delta^2/v_0)/(k_B T_c^0) = 2.0 \times 10^{-2})$ disorder. As expected, ΔS and ΔT in all cases are small except at the onset of the ferroelectric transition. For moderate disorder, ΔS increases as a result the shortening of the correlation length, while ΔT decreases as T_c shifts to lower temperatures. v_0 is the zone-center Fourier component of the dipolar force.

to the correlation length of fluctuations of polarization and not to the characteristic nanoscaled size of polar domains of relaxors.³⁸

Figures 5 (a)-(b) show ΔS and ΔT for several disorder strengths and for a fixed change in the electric field ($\Delta E_0 > 0 \rightarrow E_{cr}$). The increment in ΔS from weak-to-moderate disorder is clearly shown here together with the monotonic decrease in ΔT . For strong disorder, the ECE is weak since the dipoles are pinned by the random fields, therefore the entropy does not change significantly upon the application or removal of electric fields. Our model is qualitative and fairly good quantitative agreement with the ECE effect observed in typical relaxors where direct temperature measurements in PMN-PT show that a sharp peak in ΔT shifts to higher temperatures and increases its magnitude with increasing PT concentration (up to the morphotropic phase boundary).²⁸

Figures 5 (c)-(d) show ΔS and ΔT for several electric field strengths and for fixed (moderate) disorder. As the electric field changes increase, a broad peak develops in addition to the usual sharp one at T_c . Such broad peak in ΔT is commonly observed in relaxors and it is usually attributed to nanoscaled polar domains.^{24,28} However, our model predicts a broad peak occurs in ΔT already in the absence of compositional disorder (where there are no polar nanodomains) for very strong fields. Therefore, the broad peak is simply the expected maximum in the ECE for a ferroelectric that is deep in the supercritical

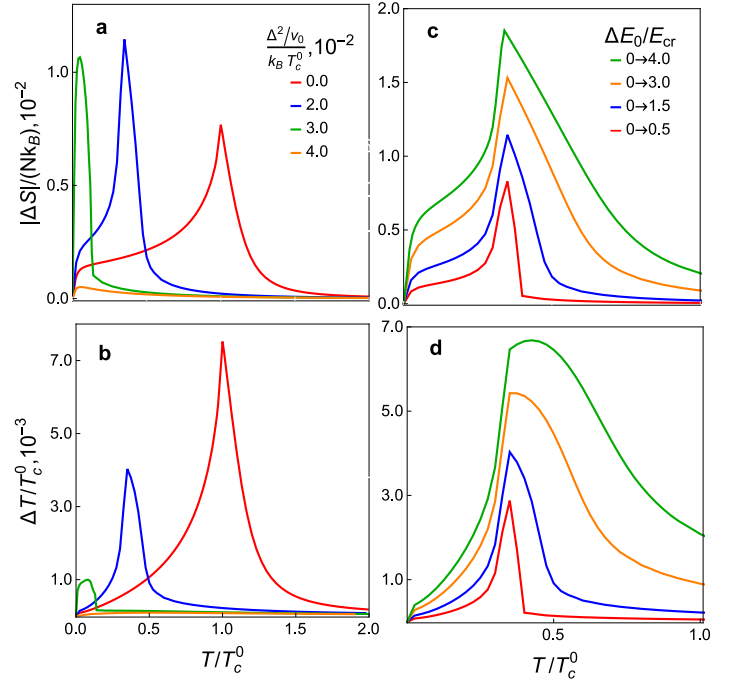


FIG. 5. (a)-(b) Calculated dependence of the ECE with compositional disorder for strong changes in the electric field $\Delta E_0/E_{cr} = 0 \rightarrow 1.5$. (c)-(d) Calculated ECE of a FE with moderate compositional disorder $((\Delta^2/v_0)/(k_B T_c^0) = 2.0 \times 10^{-2})$ for several electric field strengths.

regime, i.e., away from the critical point ($(T, E_0) \gg (T_{cr}, E_{cr})$). We obtain similar results from Landau theory (see supplement). Experimentally, this broad peak is not observed in conventional ferroelectrics as their breakdown fields are close to their critical fields, e.g., $E_{cr} \simeq 10 \text{ kV/cm}$ ³⁹ and $E_{breakdown} \simeq 14 \text{ kV/cm}$ ³⁴ for BaTiO_3 .

Starting from well-known microscopic models of ferroelectricity, we have derived a meaningful figure of merit for the ECE in a wide class of FE materials. When defining a figure of merit for a caloric effect, we find crucial to account for the well-known nonlinearities that occur near the FE transition. The large correlation lengths of fluctuations of polarization of FEs, result in a small ECE. We predict that ultraweak FEs such as those of the TSCC-family should exhibit figures of merit of about an order of magnitude larger than those of conventional displacive and order-disorder FEs. Shortening the correlation lengths

results in larger isothermal changes in entropy, lower transition temperatures, and smaller adiabatic changes in temperature. Broad peaks in the ECE such as those that have been observed in relaxors are expected for any ferroelectric that can go well into the supercritical region. Our work has implications beyond the ECE as a similar analysis could be performed for other caloric effects such as magneto- and mechano-caloric effects, which are currently being studied extensively.² Our results in combination with other recently proposed figures of merit^{40,41} should provide guidance for characterizing known caloric materials and designing new ones with enhanced performance.

Acknowledgements. We acknowledge useful discussions with Neil Mathur, Sohini Kar-Narayan, Xavier Moya, Karl Sandeman, and Chandra Varma. We thank James Scott for his comments and suggestions on the manuscript. Work at Argonne is supported by the U.S. Department of Energy, Office of Basic Energy Sciences under contract no. DE-AC02-06CH11357.

-
- ¹ S. Crossley, N. D. Mathur, X. Moya, AIP Advances **5**, 067153 (2015).
 - ² X. Moya, S. Kar-Narayan, and N. D. Mathur, Nat. Mater. **13**, 439 (2014).
 - ³ S. Pamir Alpay, J. Mantese, S. Trolier-McKinstry, Q. Zhang, and R. W. Whatmore, MRS Bulletin **39**, 1099 (2014).
 - ⁴ T. Correia and Q. Zhang (eds.), *Electrocaloric Materials: New generation of coolers* (Springer-Verlag, Berlin, 2014).
 - ⁵ M. Valant, Prog. Mater. Sci. **57**, 980 (2012).
 - ⁶ J. Scott, Annu. Rev. Mater. Res. **41**, 229 (2011).
 - ⁷ S. G. Lu and Q. M. Zhang, Adv. Mater. **21**, 1983 (2009).
 - ⁸ P. Kobeko and I. Kurchatov, Z. Phys. **66**, 192 (1930).
 - ⁹ S. Kar-Narayan and N. D. Mathur, Ferroelectrics **433**, 107 (2012).
 - ¹⁰ G. Sebald, S. Pruvost, and D. Guyomar, in *Electrocaloric Materials: New generation of coolers*, edited by T. Correia and Q. Zhang (Springer-Verlag, Berlin, 2014).
 - ¹¹ S. Kar-Narayan and N. D. Mathur, Appl. Phys. Lett. **95**, 242903 (2009).
 - ¹² Y. Jia and Y. S. Ju, Appl. Phys. Lett. **100**, 242901 (2012).
 - ¹³ H. Gu, X. Qian, X. Li, B. Craven, W. Zhu, A. Cheng, S. C. Yao, and Q. M. Zhang, Appl. Phys. Lett. **102**, 122904 (2013).
 - ¹⁴ A. S. Mischenko, Q. Zhang, J. F. Scott, R. W. Whatmore, and N. D. Mathur, Science **311**, 1270 (2006).
 - ¹⁵ B. Neese, B. Chu, S-G. Lu, Yong Wang, E. Furman, Q. M. Zhang, Science **321**, 821 (2008).
 - ¹⁶ M. E. Lines and A. M. Glass, *Principles and Applications of Ferroelectrics and Related Materials* (Clarendon Press, Oxford, 1977).
 - ¹⁷ R. Pirc, Z. Kutnjak, R. Blinc, and Q. M. Zhang J. Appl. Phys. **98**, 021909 (2011).
 - ¹⁸ L. Shebanov and K. Borman, Ferroelectrics **127**, 143 (1992).
 - ¹⁹ A. S. Mischenko, Q. Zhang, R. W. Whatmore, J. F. Scott, and N. D. Mathur, Appl. Phys. Lett. **89**, 242912 (2006).
 - ²⁰ J. Hagberg, A. Uusimäki, and H. Jantunen, Appl. Phys. Lett. **92**, 132909 (2008).
 - ²¹ T. M. Correia, J. S. Young, R. W. Whatmore, J. F. Scott, N. D. Mathur, and Q. Zhang, Appl. Phys. Lett. **95**, 182904 (2009).
 - ²² S. G. Lu, B. Rožič, Q. M. Zhang, Z. Kutnjak, R. Pirc, Minren Lin, Xinyu Li, and Lee Gorny, Appl. Phys. Lett., **97**, 202901 (2010).
 - ²³ M. Valant, Lawrence J. Dunne, Anna-Karin Axelsson, N. McN. Alford, G. Manos, J. Peräntie, J. Hagberg, H. Jantunen, and A. Dabkowski, Phys. Rev. B **81**, 214110 (2010).
 - ²⁴ L. J. Dunne, M. Valant, A. K. Axelsson, G. Manos, and N. McN. Alford, J. Phys. D: Appl. Phys. **44**, 375404 (2011).
 - ²⁵ B. Rožič, B. Malič, H. Uršič, J. Holc, M. Kosec, and Z. Kutnjak, Ferroelectrics **421**, 103 (2011).
 - ²⁶ R. Pirc, Z. Kutnjak, R. Blinc, and Q. M. Zhang J. Appl. Phys. **110**, 074113 (2011).
 - ²⁷ F. Le Goupil, A. Berenov, A. K. Axelsson, M. Valant, N. McN. Alford, J. Appl. Phys. **111**, 124109 (2012).
 - ²⁸ J. Peräntie, H. N. Taylor, J. Hagberg, H. Jantunen, and Z.-G. Ye, J. Appl. Phys. **114**, 174105 (2013).
 - ²⁹ F. Le Goupil, A.-K. Axelsson, L. J. Dunne, M. Valant, G. Manos, T. Lukasiewicz, J. Dec, A. Berenov, and N. McN. Alford Adv. Energy Mater. **4**, 1301688 (2014).
 - ³⁰ G. G. Guzmán-Verri, P. B. Littlewood, and C. M. Varma, Phys. Rev. B **88**, 134106 (2013).
 - ³¹ G. G. Guzmán-Verri, and C. M. Varma, Phys. Rev. B **91**, 144105 (2015).
 - ³² B. A. Strukov, Sov. Phys.-Crystallography **11** 757 (1967).
 - ³³ V. Franco, E. Conde, Intl. J. Refrigeration **33** 465 (2010).
 - ³⁴ K.-H. Hellwege and A. M. Hellwege Eds., *Landolt-Börnstein: Numerical Data and Functional Relationships in Science and Technology - Ferroelectrics and Related Substances* **16** (1981), Springer-Verlag Berlin.
 - ³⁵ R. Mackeviciute, M. Ivanov, J. Banys, N. Novak, Z. Kutnjak, M. Wenka, J. F. Scott, J. Phys. Condens. Matter

- 25**, 212201 (2013).
- ³⁶ S. E. Rowley, M. Hadjimichael, M. N. Ali, Y. C. Durmaz, J. C. Lashley, R. J. Cava, and J. F. Scott, arxiv:1410.2908
- ³⁷ Z. Kutnjak, R. Blinc, and Y. Ishibashi, Phys. Rev. B. **76** 104102, (2007).
- ³⁸ Y. P. Shi and A. K. Soh, Act. Mater. **59**, 5574 (2011).
- ³⁹ N. Novak, Z. Kutnjak, and R. Pirc EPL **103**, 47001 (2013).
- ⁴⁰ E. Defay, S. Crossley, S. Kar-Narayan, X. Moya and N. D. Mathur, Adv. Mater. **25**, 3337 (2013).
- ⁴¹ X. Moya, E. Defay, V. Heine, N. D. Mathur, Nature Phys. **11**, 202 (2015).

Supplemental Material - Why is the electrocaloric effect so small in ferroelectrics?

G. G. Guzmán-Verri^{1,2} and P. B. Littlewood^{3,4}

¹Materials Science Division, Argonne National Laboratory, Argonne, Illinois, USA 60439

²Centro de Investigación en Ciencia e Ingeniería de Materiales,
Universidad de Costa Rica, San José, Costa Rica 11501

³Argonne National Laboratory, Argonne, Illinois, USA 60439

⁴James Franck Institute, University of Chicago, 929 E 57 St, Chicago, Illinois, USA 60637

I. MICROSCOPIC MODEL

In this section we present the microscopic model from which we calculate the ECE. The model was recently proposed in Ref. [1] for relaxor ferroelectrics. We present it here for the sake of completeness. We focus on the relevant transverse optic mode configuration coordinate u_i of the ions in the unit cell i along the polar axis (chosen to be the z -axis). u_i experiences a local random field h_i with probability $P(h_1, h_2, \dots)$ due to the compositional disorder introduced by the different ionic radii and different valencies of, say, Mg^{+2} , Nb^{+5} , and Ti^{+4} in the typical relaxor (PMN)_{1-x}-(PT)_x. The model Hamiltonian is

$$H = \sum_i \left[\frac{\Pi_i^2}{2M} + V(u_i) \right] - \frac{1}{2} \sum_{i,j} v_{ij} u_i u_j - \sum_i h_i u_i - E_0 \sum_i u_i \quad (1)$$

where Π_i is the momentum conjugate to u_i , M is an effective mass, and E_0 is a static applied electric field. We assume the h_i 's are independent random variables with Gaussian probability distribution with zero mean and variance Δ^2 . $V(u_i) = \frac{\kappa}{2} u_i^2 + \frac{\gamma}{4} u_i^4$ is an anharmonic potential with κ, γ positive constants. $v_{ij}/e^{*2} = \begin{cases} 3 \frac{(Z_i - Z_j)^2}{|\mathbf{R}_i - \mathbf{R}_j|^5} - \frac{1}{|\mathbf{R}_i - \mathbf{R}_j|^3}, & \mathbf{R}_i \neq \mathbf{R}_j \\ 0, & \mathbf{R}_i = \mathbf{R}_j \end{cases}$ is the dipole interaction where e^* is the effective charge and Z_i is the z -component of \mathbf{R}_i . For future use, we denote $v_{\mathbf{q}} = \sum_{i,j} v_{ij} e^{i\mathbf{q} \cdot (\mathbf{R}_i - \mathbf{R}_j)}$ the Fourier transform of the dipole interaction, $v_0 (= 4\pi n z^{*2}/3)$ the $\mathbf{q} \rightarrow 0$ component of $v_{\mathbf{q}}$ in the direction transverse to the polar axis \hat{z} ($v_{\mathbf{q}}$ is non-analytic for $\mathbf{q} \rightarrow 0$), n the number of unit cells per unit volume, and a the lattice constant.

II. VARIATIONAL SOLUTION AND ENTROPY FUNCTION

In the present section, we briefly describe the variational solution of the problem posed by the Hamiltonian (1) and obtain an expression for the entropy function.

We consider a trial probability distribution, $\rho^{tr} = e^{-\beta H^{tr}}/Z^{tr}$ where $H^{tr} = \sum_i \frac{\Pi_i^2}{2M} + \frac{1}{2} \sum_{i,j} (u_i - p) G_{i-j} (u_j - p) - \sum_i h_i u_i$, is the Hamiltonian of coupled displaced harmonic oscillators in a quenched random field, and $Z^{tr} = \text{Tr} e^{-\beta H^{tr}}$ its normalization, where Π_i is

the conjugate momentum of the displacement coordinate u_i at site i and M is an effective mass.

We consider random fields $\{h_1, h_2, \dots\}$ with Gaussian probability distribution $P(h_1, h_2, \dots)$ with zero mean and variance Δ^2 . p is a uniform order parameter: it is the displacement coordinate averaged over thermal disorder first, and then over compositional disorder, $p = \int_{-\infty}^{\infty} dh_1 dh_2 \dots P(h_1, h_2, \dots) \text{Tr} \rho^{tr} u_i$; $\Omega_{\mathbf{q}}$ is the frequency of the transverse optic mode at wavevector \mathbf{q} and it is given by the Fourier transform of G_{i-j} , $M\Omega_{\mathbf{q}}^2 = \sum_{i,j} G_{i-j} e^{i\mathbf{q} \cdot (\mathbf{R}_i - \mathbf{R}_j)}$. We define $G_{i-j}^{-1} = (1/N) \sum_{\mathbf{q}} (M\Omega_{\mathbf{q}}^2)^{-1} e^{-i\mathbf{q} \cdot (\mathbf{R}_i - \mathbf{R}_j)}$. p and $\Omega_{\mathbf{q}}$ are variational parameters and are determined by minimization of the free energy $F = \int_{-\infty}^{\infty} dh_1 dh_2 \dots P(h_1, h_2, \dots) \text{Tr} \rho^{tr} [H + k_B T \ln \rho^{tr}]$.

The entropy S is given as follows,

$$\begin{aligned} \frac{S}{N} &= \int_{-\infty}^{\infty} dh_1 dh_2 \dots P(h_1, h_2, \dots) \text{Tr} \rho^{tr} (-k_B \ln \rho^{tr}) \\ &= \frac{k_B}{N} \sum_{\mathbf{q}} \left\{ \frac{\beta \hbar \Omega_{\mathbf{q}}}{2} \coth \left(\frac{\beta \hbar \Omega_{\mathbf{q}}}{2} \right) \right. \\ &\quad \left. - \ln \left[2 \sinh \left(\frac{\beta \hbar \Omega_{\mathbf{q}}}{2} \right) \right] \right\}. \quad (2) \end{aligned}$$

S depends on temperature $T = (k_B \beta)^{-1}$, the applied static field E_0 ; and the strength of compositional disorder Δ . The adiabatic changes in temperature ΔT and isothermal changes in entropy ΔS presented in the main text are calculated from Eq. (2). The correlation length of the fluctuations of polarization, ξ , is given by the frequency of the transverse optic phonon at the zone center, $\xi/a = \sqrt{(4\pi/3)\zeta/(M\Omega_0^2)}$.¹

III. BROAD PEAK IN THE ECE OF CONVENTIONAL FERROELECTRICS

In this section, we show that Landau theory predicts a broad peak in the ECE of conventional ferroelectrics. We consider the simple Landau theory of Ref. [2] for the conventional ferroelectric BaTiO_3 (BTO) in an applied field E_0 along the (001) axis. Near the the paraelectric-to-ferroelectric transition of BTO, the Landau free energy is given as follows,²

$$F = \frac{a(T - T_0)}{2} P^2 + \frac{b}{4} P^4 + \frac{c}{6} P^6 + \frac{d}{8} P^8 - PE, \quad (3)$$

where P is the polarization and $T_0 \simeq 400$ K is the supercooling temperature. The coefficients $a = 1.696 \times 10^6 \text{ Nm}^2\text{C}^{-2}$, $b = 3.422 \times 10^9 \text{ Nm}^6\text{C}^{-4}$, $c = 1.797 \times 10^{11} \text{ Nm}^{10}\text{C}^{-6}$, $d = 3.214 \times 10^{12} \text{ Nm}^{14}\text{C}^{-8}$ are determined from the dielectric susceptibility and heat capacity experiments.² The isothermal changes in temperature $\Delta T = T_2 - T_1$, are calculated self-consistently from the relation $T_2 = T_1 \exp [(a/2C) (P^2(E_2, T_2) - P^2(E_1, T_1))]$, where the temperature and electric field dependence of P are determined by the standard minimization procedure of the free energy (3). C is the contribution from the lattice to the specific heat.

In the electric field-temperature phase diagram of BTO the spinodal line begins at about $(E_0, T_c^0) \simeq (0, 405 \text{ K})$ and ends at a critical point $(E_{cr}, T_{cr}) \simeq (10 \text{ kV/cm}, 415 \text{ K})$.² The paraelectric-to-ferroelectric transition is discontinuous along the spinodal line and it is continuous at (E_{cr}, T_{cr}) . BTO is supercritical above the critical point and no transition occurs.

Figure 1 (a) shows the adiabatic changes in temperature ΔT for BTO for several changes in the field strength, ΔE_0 . ΔT exhibits a single peak at the transition point for $(\Delta E_0 \lesssim 0 \rightarrow 100 E_{cr})$, as expected. For larger ΔE_0 's than this, a broad peak develops. Clearly,

this peak cannot be observed experimentally as the required fields are well beyond BTO's breakdown electric field ($\simeq 14 \text{ kV/cm}$).³

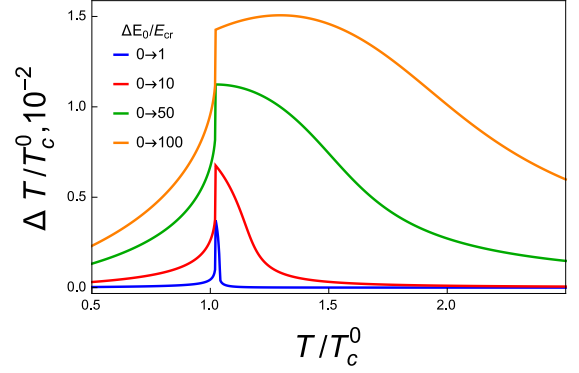


FIG. 1. Adiabatic changes in temperature, ΔT in the conventional ferroelectric BTO for several changes in the electric field strength ΔE_0 applied along the (001) direction. A secondary, broad peak arises in ΔT in addition to that at the transition temperature for very large ΔE_0 .

¹ G. G. Guzmán-Verri, P. B. Littlewood, and C. M. Varma, Phys. Rev. B **88**, 134106 (2013).

² N. Novak, Z. Kutnjak, and R. Pirc EPL **103**, 47001 (2013).

³ K.-H Hellwege and A. M. Hellwege Eds., *Landolt-Börnstein:*

Numerical Data and Functional Relationships in Science and Technology - Ferroelectrics and Related Substances **16** (1981), Springer-Verlag Berlin.